

# A ferromagnetic resonance study of as-quenched and annealed amorphous $\text{Fe}_{78}\text{Cr}_2\text{B}_{12}\text{Si}_8$

D. BAHADUR\*

*Cavendish Laboratory, Madingley Road, Cambridge CB3 0H6, UK*

RAM BILAS, PREM CHAND

*Advanced Centre for Materials Science and Department of Physics, Indian Institute of Technology, Kanpur, India*

R. A. DUNLAP

*Department of Physics, Dalhousie University, Halifax, Nova Scotia, Canada B3H 3J5*

Ferromagnetic resonance (FMR) studies of as-quenched and annealed amorphous  $\text{Fe}_{78}\text{Cr}_2\text{B}_{12}\text{Si}_8$  are presented. For short annealing times ( $\sim 30$  min) and low annealing temperatures (473 K) the resonant field,  $H_{\parallel}$  and the FMR line width,  $\Delta H$ , are essentially constant. This can be explained in terms of a combination of effects due to magnetic anisotropy and the inhomogeneous demagnetization due to stress relief in the sample. For larger annealing times or higher annealing temperatures,  $H_{\parallel}$  and  $\Delta H$  increase due to the precipitation of crystallites in the amorphous structure. X-ray diffraction, selected area electron diffraction patterns and transmission electron micrographs are consistent with this interpretation.

## 1. Introduction

Iron-based transition metal-metalloid glasses are of interest because of their unusually soft magnetic properties [1] and their superior mechanical and chemical properties [2]. Thermal treatment of these glasses produces changes in the short and long range structural ordering, and hence results in changes in the magnetic properties. Since in amorphous alloys the structural and magnetic properties are closely related, ferromagnetic resonance (FMR) is a convenient and effective method of studying these effects [3-7]. The alloy investigated in the present work,  $\text{Fe}_{78}\text{Cr}_2\text{B}_{12}\text{Si}_8$ , has been well characterized by Dunlap and co-workers, using thermal analysis [8] and Mössbauer spectroscopy [9]. In this paper we report on the results of an FMR study of the effects of various heat treatments on the properties of amorphous  $\text{Fe}_{78}\text{Cr}_2\text{B}_{12}\text{Si}_8$ .

## 2. Experimental methods

Fully amorphous alloys of the composition  $\text{Fe}_{78}\text{Cr}_2\text{B}_{12}\text{Si}_8$  were prepared by rapid quenching from the melt on to the surface of a single copper roller [10]. The resulting ribbons were approximately 1 mm wide by 20  $\mu\text{m}$  thick. The amorphous structure of these ribbons was confirmed by X-ray measurements performed on a Siemens scanning diffractometer using  $\text{MoK}\alpha$  radiation.

Room temperature FMR spectra were recorded in the X-band ( $\sim 9.4$  GHz) using a Varian E109 spectrometer. Samples were in the form of portions of

ribbons 1 mm by 2 mm cut with slow-speed diamond wheel perpendicular to the long axis of the ribbons. The samples were mounted on the flat end of a quartz rod which could be rotated about the vertical axis inside a Varian E201 rectangular cavity (unloaded  $Q \sim 7000$ ) operating in the  $\text{TE}_{102}$  mode. Spectra were recorded with the static magnetic field parallel to the plane of ribbon (in-plane) and with the static magnetic field perpendicular to the plane of the ribbon (out-of-plane). The FMR spectra were recorded as the first derivative of the absorption signal, using a 100 kHz field modulation. The incident microwave power was kept at the low value of 0.01 mW. The static magnetic field was measured using a Varian E500 digital Gauss meter and the resonant frequency was determined using a standard DPPH marker ( $g = 2.0036$ ).

Selected area diffraction (SAD) and transmission electron micrographs (TEM) were made in a Philips TEM 301 transmission electron microscope. The saturation magnetization measurements were made in an external field of 10 kG on a PAR 150 vibrating sample magnetometer (VSM). Annealing of the samples was performed *in vacuo* at temperatures ranging from 473 to 973 K for various periods of time.

## 3. Results

The derivative FMR spectra of various annealed samples in the in-plane geometry are shown in Figs 1 and 2. The principal FMR lines are broad with a typical peak-to-peak separation of a few tens of mT.

\* Permanent address: Advanced Centre for Materials Science, Indian Institute of Technology, Kanpur 20816, India

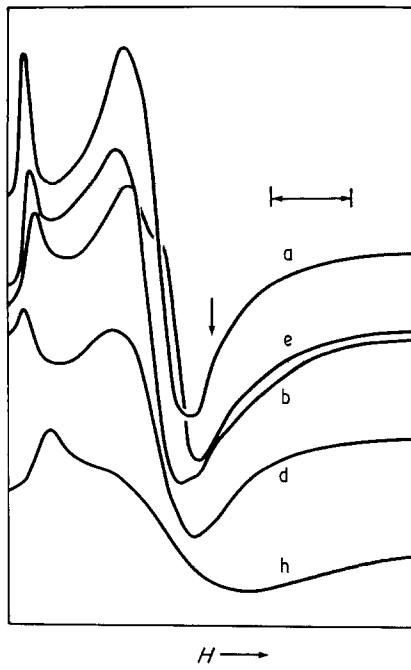


Figure 1 Room temperature FMR spectra of amorphous  $\text{Fe}_{78}\text{Cr}_2\text{B}_{12}\text{Si}_8$  samples at  $\sim 9.4$  GHz for the in-plane geometry. For annealing times and temperatures, see Table I. The reference field obtained from the calibration to DPPH (101.1 mT) is indicated by the vertical arrow; the horizontal bar corresponds to 40 mT. The spectra were obtained using different gains.

For many of the samples a very weak line is imposed on the main resonance line and appears as an additional inflection. In the present study these have been neglected. As Figs 1 and 2 illustrate, annealing appreciably affects the FMR line widths.

The conditions for in-plane and out-of-plane resonance are given by

$$(\omega/\gamma)^2 = H_{\parallel}(H_{\parallel} + 4\pi M_{\text{eff}}) \quad (1)$$

and

$$(\omega/\gamma) = H_{\perp} - 4\pi M_{\text{eff}} \quad (2)$$

respectively. Here,  $4\pi M_{\text{eff}} = 4\pi M_s - H_a$ , where  $M_s$  is the saturation magnetization and  $H_a$  is the uniaxial magnetic anisotropy field perpendicular to the plane of the sample.  $H_{\parallel}$  and  $H_{\perp}$  are the resonance fields for the in-plane and out-of-plane geometries,  $\omega$  is the microwave frequency and  $\gamma$  is the gyromagnetic ratio. The resonance field in these measurements is taken to be the zero-crossing point of the derivative absorption signal. Values of  $H_{\parallel}$  and the linewidth,  $\Delta H$ , taken to be the peak-to-peak separation of the derivative signal, are given in Table I for differently annealed samples.

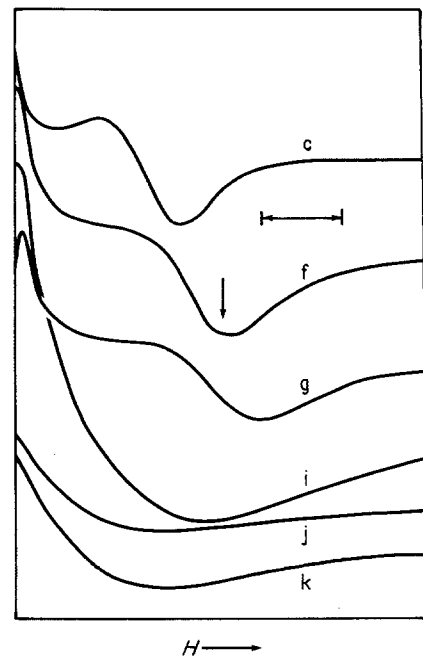


Figure 2 Additional FMR spectra for the in-plane geometry for different annealing times and temperatures (see Table I). The calibration from the DPPH marker is shown by the vertical arrow (101.1 mT); the horizontal bar corresponds to 40 mT.

Equation 1 yields values of  $\gamma$  and  $r\pi M_{\text{eff}}$  and from  $\gamma$ ,  $g$ -values can be found ( $g = 2mc\gamma/e$ ). From values of  $4\pi M_{\text{eff}}$  and the measured  $4\pi M_s$ , as determined by VSM measurements, the anisotropy field,  $H_a$ , can be obtained. These results are summarized in Table I.

SAD and TEM of the as-quenched and selected annealed samples are shown in Fig. 3. For the as-quenched sample, the SAD pattern (Fig. 3b) indicates a fully amorphous alloy and the micrograph (Fig. 3a) shows a totally homogeneous structure. The SAD pattern of the sample annealed at 573 K for 30 min (Fig. 3d) shows the alloy to be nearly amorphous. The micrograph (Fig. 3c), however, shows a significant change from the as-quenched sample and perhaps exhibits phase separation and clustering.

The SAD and TEM of the sample heated to 823 K for 5 min are shown in Figs 3e and f. This is well above the crystallization temperature of 773 K reported by Dunlap *et al* [8], and means that the sample is fully crystallized. The SAD pattern shows well defined reflections, indicating the existence of crystallinity. The grains are approximately 30 nm in diameter.

#### 4. Discussion

The resonance field and measured linewidth in FMR

TABLE I FMR and magnetization parameters for as-quenched and annealed  $\text{Fe}_{78}\text{Cr}_2\text{B}_{12}\text{Si}_8$

Sample	Annealing temperature (K)	Annealing time (min)	$H_{\parallel}$ (Oe)	$\Delta H$ (Oe)	$g$	$4\pi M_{\text{eff}}$ (FMR) (G)	$4\pi M_s$ (VSM) (G)	$H_a$ (Oe)
a		as-quenched	740	320	2.02	13760	14270	510
b	473	30	730	300	2.05	13970	14130	160
c	473	60	740	360	2.03	13760	14000	240
d	573	30	730	360	1.99	13970	14500	530
e	573	60	820	360	2.02	12270	12750	480
f	573	120	780	520	2.02	12980	13210	230
g	673	60	820	540	2.01	12270	12870	600
h	832	5	850	580	2.00	11780	12540	760

studies are due to the sum of several contributions. We write this as [11–13]

$$\omega/\gamma = H_{\text{exp}} + H_e + H_p + H_a + H_{\text{id}} \quad (3)$$

and

$$\Delta H = \Delta H_i + \Delta H_{\text{pit}} + \Delta H_e + \Delta H_p + \Delta H_{\text{id}} \quad (4)$$

where the subscripts refer to the following contributions: exp, experimental; e, eddy currents within the cavity; p, porosity; a, anisotropy; id, inhomogeneous demagnetization; i, intrinsic; and pit, pitting of the surface.

We would not expect the heat treatment to alter  $\Delta H_{\text{pit}}$ , as no surface treatment was performed. Also, we would expect  $H_e$  and  $\Delta H_e$  to be the same for all measurements. Hence the systematics of the results given in Table I should be described by the behaviour of the other components in Equations 3 and 4.

Contributions due to changes in porosity,  $p$ , should be small. Egami [14] has reported that low temperature annealing can have the effect of densifying the amorphous structure by about 1%. This results from the annealing out of vacancies and microvoids and could cause a narrowing of the FMR line given by

$\Delta H_p = 4\pi M_s \Delta p$ . In terms of the changes induced by annealing shown in Table I, this contribution is not of significance.

$H_a$  and  $\Delta H_a$  should decrease for lower annealing temperatures or shorter annealing times at moderate temperatures. This is due to the decrease in the magnetic anisotropy resulting from the decrease in the quenched-in-stress induced anisotropy. For heat treatments which are sufficient to cause cluster formation or nucleation of crystallites, we expect an increase in  $H_a$  and  $\Delta H_a$ , due to the increase in the magnetostructural anisotropy. As evidenced by Figs 2c and d, annealing at 573 K for 30 min seems to be sufficient to induce this kind of structural change. This is consistent with the measured crystallization temperature [8] and estimates of the nucleation rate based on the Arrhenius relation and typical activation energies [15].

The final contribution to  $H$  and  $\Delta H$  is from inhomogeneity. Clustering or nucleation, as is evident in Figs 2c and 3 would, through atomic migrations, enhance the short range structural inhomogeneity and would, in principle, increase  $\Delta H$  by increasing the  $\Delta H_{\text{id}}$  contribution [3, 4]. In the case of the nucleation of crystallites, crystalline regions act as inhomogeneities in the non-crystalline matrix. As shown in Table I, the

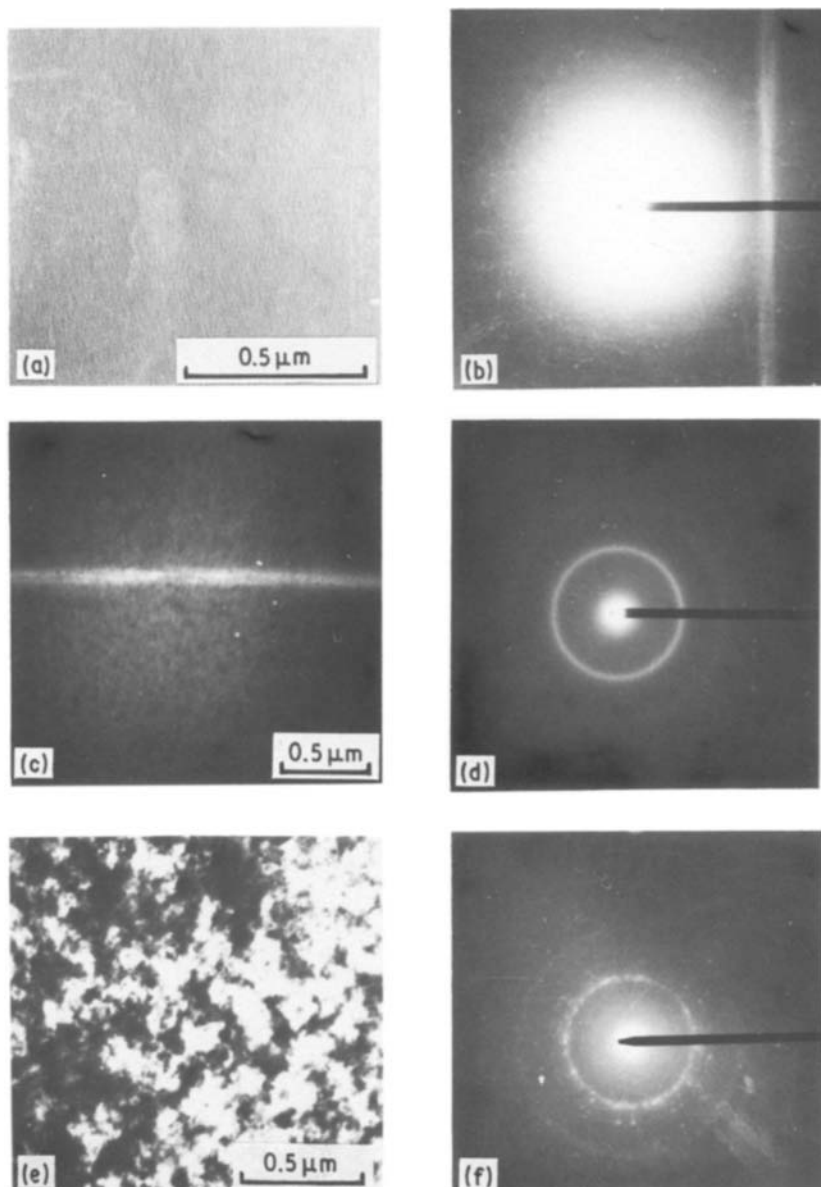


Figure 3 (a) TEM of as-quenched sample; (b) SAD of as-quenched sample; (c) TEM of sample annealed at 573 K for 30 min; (d) SAD of sample annealed at 573 K for 30 min; (e) TEM of sample annealed at 823 K for 5 min, and (f) SAD of sample annealed at 823 K for 5 min.

crystallization by annealing at high temperatures decreases the magnetization. Thus the formation of crystallites produces regions of varying magnetization and prevents the effective magnetic coupling of the amorphous regions. The significant increase in  $\Delta H$  caused by an increase in  $\Delta H_{id}$  occurs in those samples which show a significant crystallite formation in the SAD patterns. On the other hand, those samples which have been annealed at lower temperatures for shorter periods of time show neither evidence of crystallization in the SAD patterns nor an increase in  $\Delta H$ . As reported in Clogston [16], low temperature annealing can decrease the structural inhomogeneity and narrow inhomogeneously broadened FMR lines.

## 5. Conclusions

The initial near constancy observed in  $H_{||}$  and  $\Delta H$  (for low temperature annealed samples) results from a combination of effects due to magnetic anisotropy and inhomogeneous demagnetization. The rapid increase in these parameters for samples annealed at higher temperatures results from an increase in the anisotropy and the inhomogeneity as a result of an increase in clustering followed by the growth of crystallites.

## Acknowledgements

This work was supported in part by the Department of Atomic Energy, Government of India. D. Bahadur (D.B.) is grateful to the INSA-Royal Society Exchange Programme for a visiting fellowship.

## References

1. F. E. LUBORSKY (ed.) "Amorphous Metallic Alloys" (Butterworth, London, 1983).
2. R. B. DIEGLE, *J. Non-Cryst. Solids* **61-2** (1984) 601.
3. I. C. BAIANU, J. PATTERSON and K. S. RUBINSON, *Mater. Sci. Eng.* **40** (1979) 273.
4. I. C. BAIANU, K. A. RUBONSON and J. PATTERSON, *J. Phys. Chem. Solids* **40** (1979) 941.
5. D. J. WEBB and S. M. BHAGAT, *J. Magn. Magn. Mater.* **42** (1984) 109.
6. *Idem, ibid.* **42** (1984) 121.
7. S. PRASAD, R. KRISHNAN, G. SURAN, J. SZTERN, H. JOUVE and R. MEVER, *J. Appl. Phys.* **50** (1979) 1623.
8. R. A. DUNLAP, J. E. BALL and K. DINI, *J. Mater. Sci. Lett.* **4** (1985) 773.
9. R. A. DUNLAP and K. DINI, *J. Phys. F: Met. Phys.* **15** (1985) 2289.
10. R. A. DUNLAP, *Solid State Commun.* **43** (1982) 57.
11. D. BAHADUR, S. KOLLALI, C. N. R. RAO, M. J. PATNI and C. M. SRIVASTAVA, *J. Phys. Chem. Solids* **40** (1979) 981.
12. C. M. SRIVASTAVA, M. J. PATNI and N. G. NANADIKAR, *J. Phys. Colloq.* **38** (1977) C1-267.
13. C. M. SRIVASTAVA and M. J. PATNI, *J. Magn. Res.* **15** (1974) 359.
14. T. EGAMI, *Mater. Sci. Eng.* **32** (1978) 293.
15. M. G. SCOTT, in "Amorphous Metallic Alloys", edited by F. E. Luborsky (Butterworth, London, 1983) p. 144.
16. A. M. CLOGSTON, *J. Appl. Phys.* **29** (1958) 334.

*Received 6 August  
and accepted 22 September 1986*